

A methyl-seq tool to capture genomic imprinted loci

Hubert Jean-Noël^{1*}, Iannuccelli Nathalie^{1*}, Cabau Cédric², Jacomet Eva^{1,3}, Billon Yvon⁴, Serre Rémy-Felix^{5,6}, Vandecasteele Céline⁵, Donnadiou Cécile⁵, Demars Julie^{1*}

¹GenPhySE, Université de Toulouse, INRAE, ENVT, F-31326 Castanet-Tolosan, France

²Sigenae, GenPhySE, Université de Toulouse, INRAE, ENVT, F-31326 Castanet-Tolosan, France

³ENVT, F-31326 Castanet-Tolosan, France

⁴GenESI, INRAE, F-17700, Surgères, France (<https://doi.org/10.15454/1.5572415481185847E12>)

⁵INRAE, GeT-PlaGe, Genotoul, F-31326 Castanet-Tolosan, France (<https://doi.org/10.15454/1.5572370921303193E12>)

⁶Qualyse, Le Treuil, INRAE, 19000, Tulle, France

*equal contribution

†corresponding author: julie.demars@inrae.fr

Genomic imprinting represents an original model of epigenetic regulation resulting in a parent-of-origin expression. Despite the critical role of imprinted genes in mammalian growth, metabolism and neuronal function, there is no molecular tool specifically targeting them for a systematic evaluation. Here, we optimized and compared to bisulfite-based standard a novel methyl-seq system to capture 165 candidate regions for genomic imprinting and ultimately detect parent-of-origin methylation, the main hallmark of imprinting.

Genomic imprinting (GI) is an original molecular phenomenon mediated by the apposition of epigenetic marks (DNA methylation and/or histone marks) leading to allele-specific expression dependent on the parental origin¹. GI studies intersect with a broad range of biological fields, including evolution biology, developmental biology, molecular genetics and epigenetics. GI is involved in many phenotypes in humans but also contributes to the variability of major agronomic phenotypes^{2,3}. Imprinted genes are therefore highly attractive targets and biomarkers^{4,5}, which are found isolated or as clusters across the genome, representing 1% to 2% of the total gene content in the best studied mammals. Parent-of-origin (PofO) expression is primarily controlled by differentially methylated regions (DMRs) in a parental way as well¹. Although knowledge about GI has significantly advanced so far, some technological bottlenecks remain to tackle challenging scientific insights.

To assess whether and how GI is involved in the variability of complex phenotypes, it is critical to (i) map and characterize imprinted loci across the genome and (ii) identify simultaneously the parental origin of alleles and their methylation status. Rigorously characterizing imprintomes would require the combination of experimental designs such as reciprocal crosses⁶ with genome-scale sequencing technologies^{7,8}. However, such cost-consuming methods could not be used as routine molecular tools. Here, we optimized and compared capture-based methylation sequencing technologies aiming for imprinted loci across the genome.

We performed our study in the pig (*Sus scrofa*) because porcine GI is largely under-characterized, despite wide-ranging implications not limited to the improvement of major agronomical phenotypes^{9,10}. The strategy implemented below may be applied to any other species with its own custom capture. We (i) selected 165 regions in the pig genome based on human and mouse orthologies^{1,11} (<https://www.geneimprint.com> and <https://corpapp.otago.ac.nz/gene-catalogue>), since GI mechanisms are quite well conserved in mammals¹², (ii) exploited reciprocal crosses to identify PofO methylation⁶ and (iii) tested two different technologies, the novel Twist NGS Bioscience Methylation Detection System (TB), with two protocols (called TB1 and TB2), and the widely used Agilent SureSelect Custom DNA Target Enrichment Probes (AG) (Fig. 1a and Extended Data Table 1)¹³.

The final designed panels from both technologies covered all the 165 targeted regions but differed slightly in size, with 20.5 Mb and 19.7 Mb for TB and AG technologies, respectively (Fig. 1b and Extended Data Table 1). Sequencing quality analysis showed lower duplication rate and higher GC percentage for TB technology in addition to insert size as expected (Fig. 1c-e and Extended Data Fig. 1a-h). Both target capture efficiency and homogeneity of panels

52 are comparable between AG and TB after optimizing the latter, reaching excellent levels (Fig. 1f and g). Specificity is
53 however more favourable in TB, with much less off-target capture than in AG (Fig. 1h and i and Extended Data Fig.
54 1g-i). About methylation evaluation and conversion, the enzymatic-based TB technology yielded higher numbers of
55 total and methylated CpGs, as well as less non-CpG methylation than the standard bisulfite-based AG technology
56 (Extended Data Fig. 1j-n). In addition, we demonstrated better capture of GC-rich regions with TB technology,
57 including CpG islands, independently of region size (Fig. 1j-l). Thus, the application of the novel TB approach to GI
58 suggests it outperforms the current technological standard for methylation quantification¹³.
59 Imprinted genes are regulated by CpG methylation through parental DMRs¹⁴. Such hemi-methylated regions,
60 expected to be methylated on one allele resulting in approximately 50% of methylation, are either somatic or
61 germinal¹⁵. Here, we identified approximately 38,000 hemi-methylated CpGs per individual, clustered in at least 600
62 DMRs fulfilling stringent criteria that are distributed in 123 out of the 165 candidate regions (Fig. 2a-c). Interestingly,
63 the *IGF2-H19/KCNQ1-CDKN1C* region, carrying a mutation affecting muscularity in pigs¹⁶ and hosting some of the
64 best-characterized Imprinting Control Regions (ICRs) in humans and mice¹⁷, is the top candidate after scanning for
65 GI methylation patterns. Two clusters with more than 100 hemi-methylated CpGs were detected in the region. The
66 first one is located upstream of the 5' UTR of *H19* and the second one is located upstream of the 5'UTR of *KCNQ1OT1*
67 that is not annotated in the pig reference genome (Fig. 2e-h).
68 Our strategy relies on next generation sequencing technology that allows the detection of genotypes and CpG
69 methylation simultaneously. Reciprocal crosses were used to phase variants and determine unambiguously the
70 parental inheritance of alleles (Fig. 2i-l and Extended Fig.2a). We demonstrated, in blood, the paternal specific
71 methylation for the DMR located upstream of the 5' UTR of *H19* and the maternal specific methylation for the DMR
72 located upstream of the 5' UTR of *KCNQ1OT1* (Fig. 2m and n and Extended Fig.2a-c). This result was confirmed on
73 a sperm sample in which the first region was totally methylated while the second one was totally unmethylated (Fig.
74 2m and n). Both germline DMRs showed similar properties than ICR1 and ICR2, which are known to regulate in
75 humans and mice the *IGF2-H19* and *KCNQ1-CDKN1C* imprinted domains, respectively^{1,18,19}.
76 Altogether, we demonstrated and harnessed the potential of the Twist NGS Bioscience Methylation Detection System
77 to provide a molecular tool adapted to the specific needs of GI. Such a novel tool especially allows detecting PofO
78 methylation, which paves the way to the systematic and routine evaluation of the contribution of GI in both the
79 variability of livestock complex phenotypes⁵ and the diagnosis of human imprinting disorders^{2,7}.

80
81

82 **Methods**

83 *Animals and Samples*

84 The study included 10 pigs, 8 pigs were bred at the INRAE experimental farm
85 (<https://doi.org/10.15454/1.5572415481185847E12>) and 2 pigs come from breeding organizations in accordance with
86 the French and European legislation on animal welfare. The animals belong to the same family, except for one LW
87 animal. Animals were produced in a reciprocal cross design between Large White and Meishan pig breeds.

88 Ten biological samples were used in the experiment. Nine of them are blood samples collected on EDTA and were
89 stored frozen nine months at -20°C. One biological sample is a sperm sample from dose for artificial insemination
90 and was stored two years at -20°C. Biological samples were collected at adult developmental stage for all the parents
91 (n=5) of the reciprocal cross design while biological samples were collected at 1d after birth for all offspring (n=5) of
92 the reciprocal cross design.

93 Genomic DNA was extracted from blood using the Genomic-tip 100 DNA kit (Qiagen, 10243) or using MagAttract
94 HMW DNA kit (Qiagen, 67563) following manufacturer's instructions. Genomic DNA was extracted from sperm
95 using standard phenol/chloroform method. DNA purity was determined using the Nanodrop 8000
96 spectrophotometer (Thermo Fisher Scientific). DNA concentration was determined using the DS DNA Broad Range
97 Assay kit (Invitrogen, ThermoFisher Scientific, Q32850) and was measured with the Qubit3 fluorometer (Invitrogen,
98 ThermoFisher Scientific).

99 All the procedures and guidelines for animal care were approved by the local ethical committee in animal
100 experimentation (Poitou-Charentes) and the French Ministry of Higher Education and Scientific Research
101 (authorizations n°2018021912005794 and n°11789-2017101117033530). All information about animals and samples
102 are available at ENA under study accession PRJEB58558.

103

104 **Panel design**

105 Candidate regions for GI in the pig (*Sus scrofa*) were selected based on various publications available in humans and
106 mice^{1,11} and on two databases (<https://www.geneimprint.com> and <https://corpapp.otago.ac.nz/gene-catalogue>). A
107 total of 165 regions ranging from 458 bp to 2.3 Mb, distributed across the 18 autosomes, the X chromosome and 4
108 scaffolds of the pig reference genome Sscrofa11.1, were selected. These genomic regions, targeting a total of 23 Mb,
109 were submitted to the two commercial platforms, TB and AG. Each platform used its own confidential algorithm for
110 panel design. The sizes of custom panels from TB and AG were 20.5 Mb and 19.7 Mb, respectively, with all the 165
111 candidate regions for GI represented.

112 **Library preparation**

113 The final optimized protocol has been deposited to Protocol Exchange open repository
114 (<https://doi.org/10.21203/rs.3.pex-2159/v1>).

115 Two types of libraries were generated using AG or TB technology, the latter involving two experiments (TB1 and
116 TB2). The AG and the TB1 experiments were performed at the GeT-PlaGe core facility at INRAE Toulouse
117 (<https://doi.org/10.15454/1.5572370921303193E12>). The TB2 experiment was performed by Twist Bioscience company
118 (Twist Bioscience, USA).

119 *Library preparation and target enrichment with Agilent SureSelect Custom DNA Target Enrichment Probes*

120 Eight library preparations were carried out using the SureSelect Methyl-Seq Target Enrichment kit (Agilent, G9651)
121 following the manufacturer's protocol (User guide: SureSelect, Agilent Technologies, version E0, April 2018).
122 Genomic DNA (1µg) was first fragmented using a Covaris M220 focused ultrasonicator in micro-TUBE 50 AFA Fiber
123 screw cap (Covaris, 520166) for a target insert size of 200 bp under the following conditions: peak power 75W, duty
124 factor 10%, 200 cycles/bursts, 375s, 8°C. An additional 0.8X AMPure beads purification step was done to eliminate
125 adaptor dimers.

126 *Library preparation and target enrichment with Twist Bioscience NGS Methylation Detection System*

127 Sixteen library preparations were carried out using an in-house combination of two protocols: NEB-Next Enzymatic
128 Methyl-seq Library Preparation and Twist Bioscience Targeted Methylation Sequencing, using a methyl custom
129 panel. The whole detailed and optimized protocol has been deposited to Protocol Exchange open repository
130 (<https://doi.org/10.21203/rs.3.pex-2159/v1>). Briefly, eight library preparations were carried out with a first similar
131 development protocol (TB1) in which some adjustments have not yet been made. Differences between protocol^{TB1}
132 and protocol^{TB2} are referenced in the procedure deposited in Protocol Exchange. All library quantifications were
133 performed on a Qubit 3.0 fluorometer with High Sensitivity DNA Quantitation Assay kit according manufacturer's
134 recommendations (Agilent, ThermoFisher Scientific, Q32851). All library validations were performed on a 2100
135 Bioanalyzer with High Sensitivity DNA kit according to manufacturer's recommendations (Agilent Technologies,
136 5067-4626).

137 **Sequencing**

138 All libraries were quantified by qPCR on QuantStudio 6 device (Applied Biosystems, ThermoFisher Scientific), using
139 the Kapa Library Quantification Kit (Roche, KK4824). Agilent libraries and experiment TB1 libraries were each
140 sequenced on one lane of an Illumina SP NovaSeq 6000 flow cell, using the SP Reagent kit v1.5 300 cycles (Illumina,
141 20028400), according to the manufacturer's recommendations. The loading concentration was 2 nM 25% phiX.
142 Experiment TB2 libraries were sequenced on Illumina P2 NextSeq 2000 flow cell, using the SP Reagent kit v3 300
143 cycles (Illumina, 20046813), according to the manufacturer's recommendations. The loading concentration was 1000
144 pM 5% phiX. All sequences are available at ENA under study accession PRJEB58558.

145 **Methyl-seq data analysis**

146 Analyses were performed using the genotoul bioinformatics platform Toulouse Occitanie (Bioinfo Genotoul,
147 <https://doi.org/10.15454/1.5572369328961167E12>). Methyl-seq reads were processed with the nf-core/methylseq
148 (v1.5) pipeline^{20,21} (<https://nf-co.re/methylseq>), using the Sscrofa11.1 pig reference and the Bismark²² workflow with
149 standard parameters. Sequencing quality analysis was performed with custom Python scripts. CpG calls with DP ≥
150 20 were further processed with CGmapTools²³ and inbuilt Linux commands. Cytosines with methylation levels either
151 < 0.3 or > 0.7 were classified as either hypo-methylated or hyper-methylated, respectively. Cytosines with
152 methylation levels between 0.4 and 0.6, indicating potential PofO methylation, were classified as hemi-methylated.
153 This subset of hemi-methylated CpGs was scanned using a sliding window approach with a custom R function to
154 identify candidate DMRs compatible with GI. The occurrence of ≥ 5 hemi-methylated CpGs within 100 bp was
155 labelled as DMR100. The upper fraction of DMR100, that is the occurrence of ≥ 5 consecutive hemi-methylated CpGs,
156

159 was further prioritized and labelled as DMR5, which happens to 0.2% of hemi-methylated CpGs. All of these criteria
160 correspond to the strictest standards currently used when looking for epigenetic signatures of GI7. Neighbouring
161 DMRs at a distance less than their initial definition criterion (i.e., 100 bp for DMR100 and 5 bp for DMR5) were
162 merged in a single larger DMR. Top DMRs were visually inspected using Integrative Genomics Viewer²⁴. A complete
163 list of software versions used in this study is provided in the next section.

164

165 *Software used*

166 BEDtools (v2.27.1)²⁵

167 Bismark (v0.22.3)²²

168 CGmapTools (v0.1.2)²³

169 Cutadapt (v2.9)²⁶

170 nf-core/methylseq (v1.5)^{20,21}

171 Nextflow (v20.01.0)²⁷

172 FastQC (v0.11.9, <https://www.bioinformatics.babraham.ac.uk/projects/fastqc/>)

173 Integrative Genome Viewer (v2.8.13)²⁴

174 MultiQC (v1.8)²⁸

175 Qualimap (v2.2.2-dev)²⁹

176 Preseq (v2.0.3)³⁰

177 R base (v4.1.1) with dplyr (v1.0.9), ggplot2 (v3.3.6), RIdeogram (v0.2.2), scales (v1.2.1) and tidyr (v1.2) packages

178 (<https://cran.r-project.org/>).

179 Samtools (v1.9)³¹

180 Trim Galore! (v0.6.4_dev, https://www.bioinformatics.babraham.ac.uk/projects/trim_galore/)

181 HISAT2 (v2.2.0)³²

182

183 **Data availability**

184 All information about animals, samples and raw sequences are available at ENA under study accession PRJEB58558.

185 The optimized final step-by-step protocol, TB2, has been deposited to Protocol Exchange open repository

186 (<https://doi.org/10.21203/rs.3.pex-2159/v1>).

187

188 **Acknowledgements**

189 We are grateful to the genotoul bioinformatics platform Toulouse Occitanie (Bioinfo Genotoul,

190 <https://doi.org/10.15454/1.5572369328961167E12>) for providing computing and storage resources. We are grateful to

191 the genotoul GeT-PlaGe platform Toulouse Occitanie (GeT Genotoul,

192 <https://doi.org/10.15454/1.5572370921303193E12>) for providing resources and sequencing facilities. We are grateful

193 to people from the INRAE experimental farm (<https://doi.org/10.15454/1.5572415481185847E12>) who took care of

194 animals. We are grateful to people from Agilent, New England Biolabs and Twist Bioscience for support throughout

195 the optimization. Finally, we are grateful to S. Leroux, A. Lakhali and M. Perret for their punctual help.

196

197 **Funding**

198 This protocol was funded by the ANR PIPETTE (ANR-18-CE20-0018) and FEDER-FSE SeqOccIn projects. Jean-Noël

199 Hubert is partly funded by the ANR PIPETTE and the Animal Genetics division of INRAE.

200

201 **Author Information**

202 These authors contributed equally: Jean-Noël Hubert and Nathalie Iannuccelli

203 *Authors and Affiliations*

204 GenPhySE, Université de Toulouse, INRAE, ENVT, F-31326 Castanet-Tolosan, France

205 Jean-Noël Hubert, Nathalie Iannuccelli and Julie Demars

206 Sigénae, GenPhySE, Université de Toulouse, INRAE, ENVT, F-31326 Castanet-Tolosan, France

207 Cédric Cabau

208 ENVT, F-31326 Castanet-Tolosan, France

209 Eva Jacomet

210 GenESI, INRAE, F-17700, Surgères, France (<https://doi.org/10.15454/1.5572415481185847E12>)

211 Yvon Billon

212 INRAE, GeT-PlaGe, Genotoul, F-31326 Castanet-Tolosan, France (<https://doi.org/10.15454/1.5572370921303193E12>)
213 Rémy-Félix Serre, Céline Vandecasteele and Cécile Donnadiou
214 Qualyse, Le Treuil, INRAE, 19000, Tulle, France

215 Rémy-Félix Serre

216 **Contributions**

217 J.N.H. analysed methylation data and wrote the manuscript, I.N. performed the experiments and wrote the protocol
218 submitted to Protocol Exchange, R.F.S. performed the experiments, C.C. and C.V. analysed raw quality sequencing
219 data, E.J. conducted analyses and visualization for the *IGF2-H19/KCNQ1-CDKN1C* region, Y.B. provided animals,
220 C.D. acquired funding and J.D. supervised the project, acquired funding, analysed data and wrote the manuscript.

221 **Corresponding authors**

222 Correspondence to Julie Demars

223

224 **Ethics declarations**

225 **Competing interests**

226 The authors declare no competing interests.

227

228

229 **References**

- 230 1. Tucci, V. *et al.* Genomic Imprinting and Physiological Processes in Mammals. *Cell* **176**, 952–965 (2019).
- 231 2. Monk, D., Mackay, D. J. G., Eggermann, T., Maher, E. R. & Riccio, A. Genomic imprinting disorders: lessons on
232 how genome, epigenome and environment interact. *Nat Rev Genet* **20**, 235–248 (2019).
- 233 3. O'Doherty, A. M., MacHugh, D. E., Spillane, C. & Magee, D. A. Genomic imprinting effects on complex traits in
234 domesticated animal species. *Frontiers in Genetics* **6**, 156 (2015).
- 235 4. Shen, R. *et al.* Novel visualized quantitative epigenetic imprinted gene biomarkers diagnose the malignancy of
236 ten cancer types. *Clinical Epigenetics* **12**, 71 (2020).
- 237 5. Ibeagha-Awemu, E. M. & Zhao, X. Epigenetic marks: regulators of livestock phenotypes and conceivable sources
238 of missing variation in livestock improvement programs. *Frontiers in Genetics* **6**, (2015).
- 239 6. Edwards, C. A. *et al.* Weak parent-of-origin expression bias: Is this imprinting? 2022.08.21.504536 at
240 <https://doi.org/10.1101/2022.08.21.504536> (2022).
- 241 7. Jima, D. D. *et al.* Genomic map of candidate human imprint control regions: the imprintome. *Epigenetics* **17**, 1920–
242 1943 (2022).
- 243 8. Akbari, V. *et al.* Genome-wide detection of imprinted differentially methylated regions using nanopore
244 sequencing. *eLife* **11**, e77898 (2022).
- 245 9. O'Brien, E. K. & Wolf, J. B. Evolutionary Quantitative Genetics of Genomic Imprinting. *Genetics* **211**, 75–88 (2019).
- 246 10. Lu, X. *et al.* Evolutionary epigenomic analyses in mammalian early embryos reveal species-specific innovations
247 and conserved principles of imprinting. *Sci. Adv.* **7**, eabi6178 (2021).
- 248 11. Gigante, S. *et al.* Using long-read sequencing to detect imprinted DNA methylation. *Nucleic Acids Research* **47**,
249 e46–e46 (2019).
- 250 12. Kaneko-Ishino, T. & Ishino, F. The Evolutionary Advantage in Mammals of the Complementary Monoallelic
251 Expression Mechanism of Genomic Imprinting and Its Emergence From a Defense Against the Insertion Into the
252 Host Genome. *Frontiers in Genetics* **13**, (2022).
- 253 13. Tanić, M. *et al.* Comparison and imputation-aided integration of five commercial platforms for targeted DNA
254 methylome analysis. *Nat Biotechnol* **40**, 1478–1487 (2022).
- 255 14. Noordermeer, D. & Feil, R. Differential 3D chromatin organization and gene activity in genomic imprinting.
256 *Current Opinion in Genetics & Development* **61**, 17–24 (2020).
- 257 15. Kobayashi, H. Canonical and Non-canonical Genomic Imprinting in Rodents. *Front. Cell Dev. Biol.* **9**, 713878
258 (2021).
- 259 16. Van Laere, A.-S. *et al.* A regulatory mutation in *IGF2* causes a major QTL effect on muscle growth in the pig.
260 *Nature* **425**, 832–836 (2003).
- 261 17. Shmela, M. E. & Gicquel, C. F. Human diseases versus mouse models: insights into the regulation of genomic
262 imprinting at the human 11p15/mouse distal chromosome 7 region. *J Med Genet* **50**, 11–20 (2013).
- 263 18. Barlow, D. P. & Bartolomei, M. S. Genomic Imprinting in Mammals. *Cold Spring Harb Perspect Biol* **6**, a018382
264 (2014).

- 265 19. Maupetit-Méhouas, S. *et al.* Imprinting control regions (ICRs) are marked by mono-allelic bivalent chromatin
266 when transcriptionally inactive. *Nucleic Acids Res* **44**, 621–635 (2016).
- 267 20. Ewels, P. A. *et al.* The nf-core framework for community-curated bioinformatics pipelines. *Nat Biotechnol* **38**, 276–
268 278 (2020).
- 269 21. Ewels, P. *et al.* *nf-core/methylseq: nf-core/methylseq version 1.5 [Belated Dodo]*. (Zenodo, 2020).
270 doi:10.5281/ZENODO.3746458.
- 271 22. Krueger, F. & Andrews, S. R. Bismark: a flexible aligner and methylation caller for Bisulfite-Seq applications.
272 *Bioinformatics* **27**, 1571–1572 (2011).
- 273 23. Guo, W. *et al.* CGmapTools improves the precision of heterozygous SNV calls and supports allele-specific
274 methylation detection and visualization in bisulfite-sequencing data. *Bioinformatics* **34**, 381–387 (2018).
- 275 24. Thorvaldsdóttir, H., Robinson, J. T. & Mesirov, J. P. Integrative Genomics Viewer (IGV): high-performance
276 genomics data visualization and exploration. *Briefings in Bioinformatics* **14**, 178–192 (2013).
- 277 25. Quinlan, A. R. & Hall, I. M. BEDTools: a flexible suite of utilities for comparing genomic features. *Bioinformatics*
278 **26**, 841–842 (2010).
- 279 26. Martin, M. Cutadapt removes adapter sequences from high-throughput sequencing reads. *EMBnet j.* **17**, 10
280 (2011).
- 281 27. Di Tommaso, P. *et al.* Nextflow enables reproducible computational workflows. *Nat Biotechnol* **35**, 316–319 (2017).
- 282 28. Ewels, P., Magnusson, M., Lundin, S. & Käller, M. MultiQC: summarize analysis results for multiple tools and
283 samples in a single report. *Bioinformatics* **32**, 3047–3048 (2016).
- 284 29. Okonechnikov, K., Conesa, A. & García-Alcalde, F. Qualimap 2: advanced multi-sample quality control for high-
285 throughput sequencing data. *Bioinformatics* **32**, 292–294 (2016).
- 286 30. Daley, T. & Smith, A. D. Predicting the molecular complexity of sequencing libraries. *Nat Methods* **10**, 325–327
287 (2013).
- 288 31. Danecek, P. *et al.* Twelve years of SAMtools and BCFtools. *GigaScience* **10**, giab008 (2021).
- 289 32. Kim, D., Paggi, J. M., Park, C., Bennett, C. & Salzberg, S. L. Graph-based genome alignment and genotyping with
290 HISAT2 and HISAT-genotype. *Nat Biotechnol* **37**, 907–915 (2019).
- 291
- 292

293 Figure legends

294 **Fig.1: Strategy and performances of technologies.** **a**, Schematic overview of the strategy, including the selection of
295 165 candidate regions for GI in the pig based on knowledge from humans and mice^{1,11}, the use of a reciprocal cross
296 (n=8) to ensure the determination of parental inheritance⁶ and the tested technologies, Twist Bioscience (TB) *vs.*
297 Agilent (AG). **b**, Distribution and size of final designed panels by the two manufacturers, AG (green), TB (purple),
298 and uncovered regions (grey). **c, d, e**, Sequencing performances by technology, including insert size (**c**), duplication
299 rate (**d**) and GC percentage (**e**). **f, g, h, i**, Panel performances by technology, including efficiency, that is represented
300 as the mean +/- standard deviation of the fraction of targets covered at a specific depth (**f**), homogeneity, that is
301 represented as the mean +/- standard deviation of depth coverage for the 165 targeted regions (**g**), specificity, that is
302 represented as percentage (**h**) and density (**i**) of off-target reads, which mapped outside of the 165 targeted regions.
303 **j, k**, Correlation of the mean coverage with either the size (**j**) or the GC percentage (**k**) of the 165 targeted regions.
304 For **c** to **k**, the AG classical protocol is in green and the two TB protocols (TB1 and TB2) are in light and dark purple.
305 **l**, Feature annotation of region per technology.

306

307 **Fig.2: Hemi-methylated CpGs, DMRs and PofO methylation.** Results showed here come from the TB2 protocol. **a**,
308 Detection, methylation and classification of CpGs. The methylation at CpGs was considered hyper/hypo/hemi when
309 methylation was <70%, >30% and between 40% and 60%, respectively. **b**, Repartition of hyper/hypo/hemi-methylated
310 CpGs in the 165 candidate regions for GI. **c**, Location of the DMRs across the pig genome. **d**, Schematic representation
311 of the *IGF2-H19/KCNQ1-CDKN1C* imprinted region located on the swine chromosome 2 with genes expressed from
312 the paternal and maternal allele in blue and red, respectively. **e, f**, Magnification of two regions where two clusters
313 of hemi-methylated CpGs, DMRs (pink), were detected. Locally weighted running lines smoother (LOESS) were
314 represented. **g** to **n**, Screenshots from IGV browser (<https://software.broadinstitute.org/software/igv/>) magnified in
315 DMRs. **g, h**, Annotation of the pig genome using *Sus_scrofa.Scrofa11.1.104.gtf* showing that *KCNQ1OT1* was
316 missing. **i, j**, Coverage. **k, l**, Variants identification and informativity with parental origin in the offspring of
317 reciprocal crosses. **n, m**, Methylation evaluation in blood and sperm tissues and detection of PofO methylation.

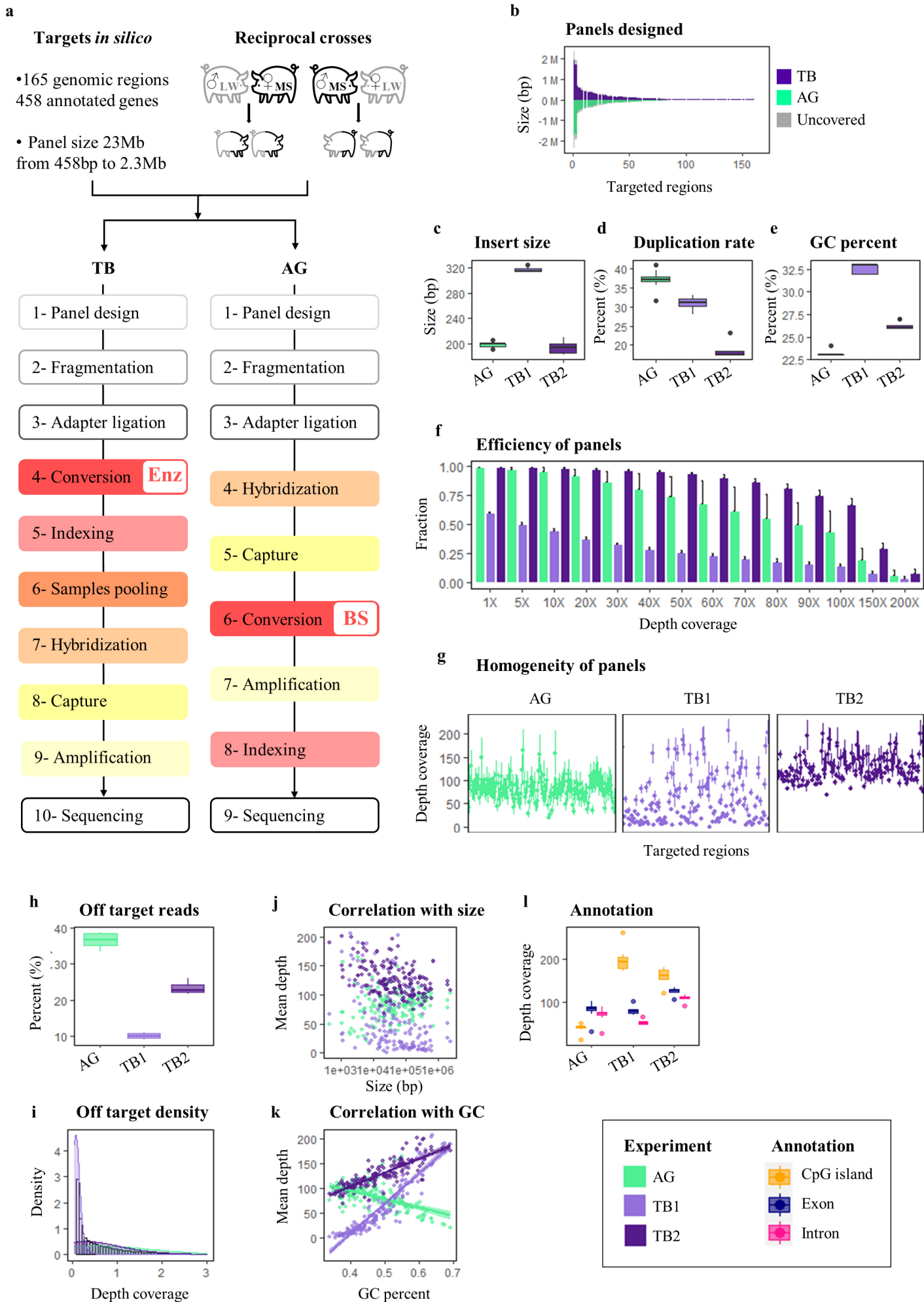


Figure 1

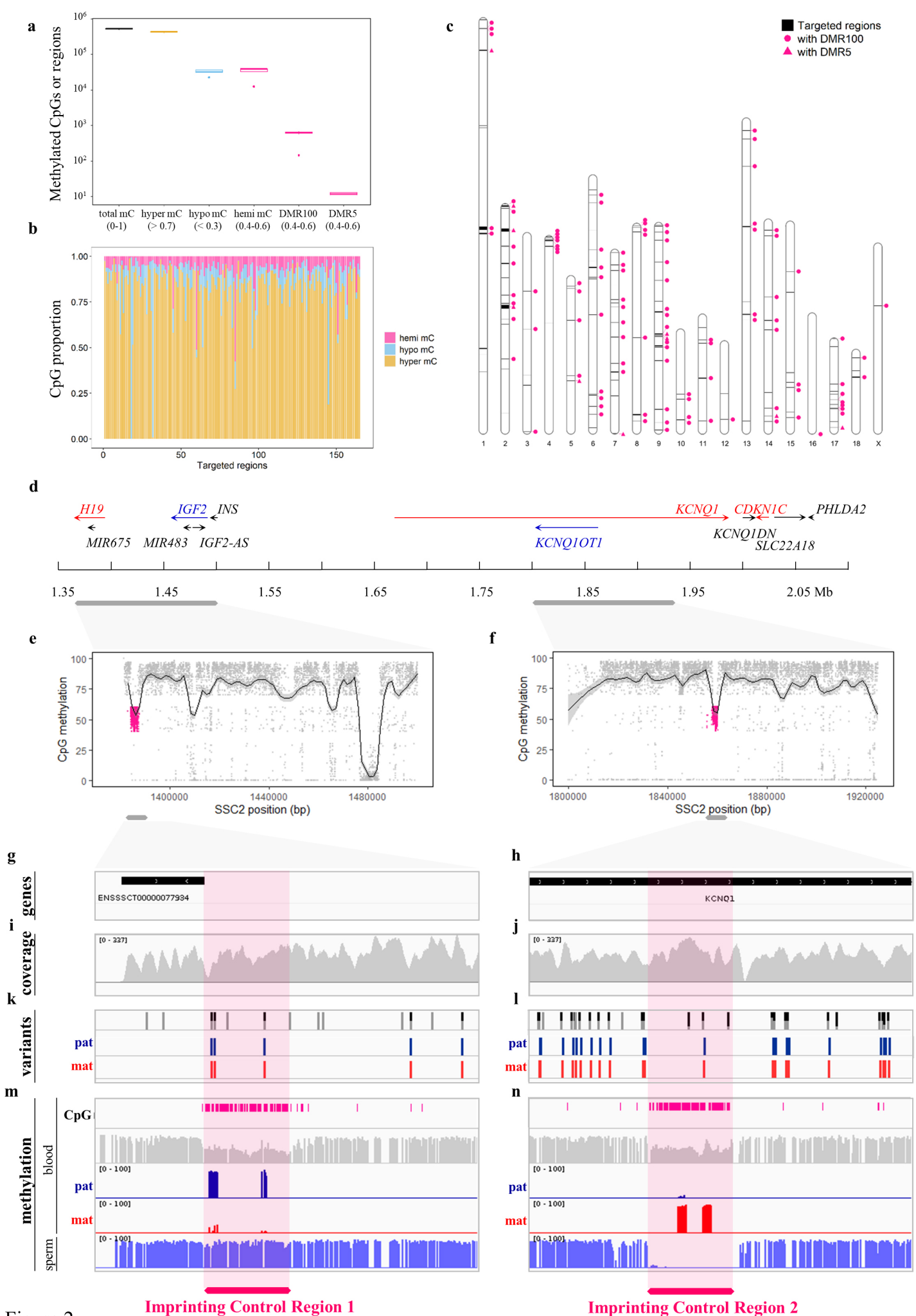
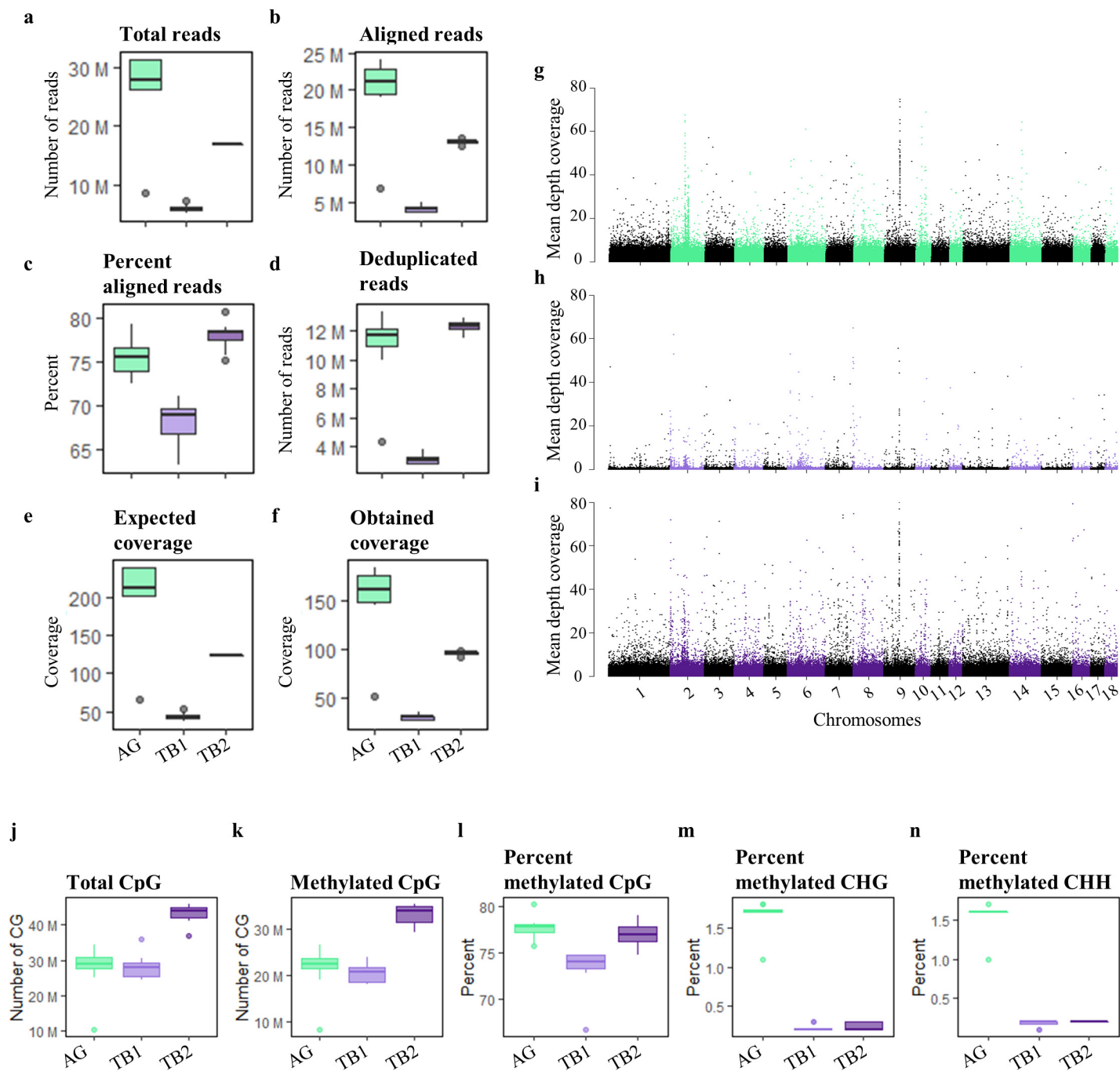


Figure 2

	TB	AG
Input DNA	200 ng	1 µg
Conversion	Enzymatic	Chemical
Methylation step	Pre-capture	Post-capture
Hybridization probes	dsDNA methylated	RNA
Libraries	Pooling of 8	Individual
Indexing	384	96
Probes number	170,792	314,240
Panel designed	20,488,283 bp (87%)	19,687,287 bp (84%)

Extended Data Table 1: Main differences between the tested technologies. The AG technology and protocol correspond to the widely used AG SureSelect Custom DNA Target Enrichment Probes. The TB technology and protocols correspond to the novel Twist NGS Bioscience Methylation Detection System. TB=Twist Bioscience, AG=Agilent

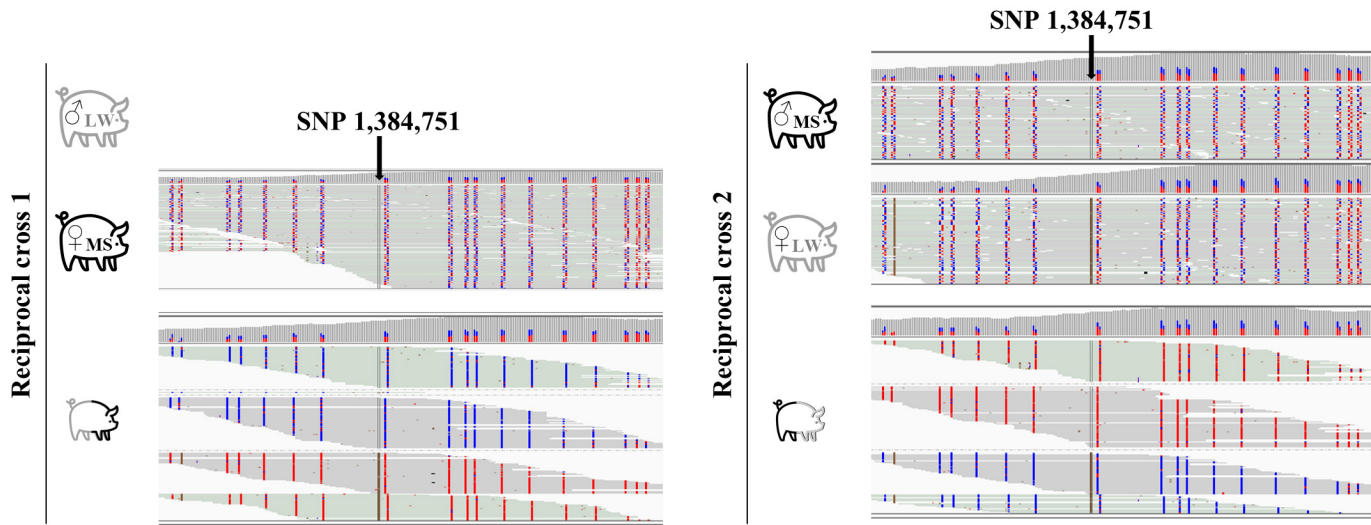


Extended Data Fig.1: Additional performances of the tested technologies. The AG classical protocol is in green and the two tested protocols for TB are in light and dark purple. The reference used is Sscrofa11.1 (GCA_000003025.6). The methylation pipeline analysis used is the module nf-core/methylseq from nf-core-Nextflow-v20.01.0. **a to f**, Sequencing performances by technology, including number of reads generated per technology (**a**), number of reads mapped on the reference genome (**b**), percentage of mapped reads (**c**), number of deduplicated reads (**d**), expected (**e**) and final (**f**) coverage. **g, h, i**, Distribution of off-target reads across the pig genome. The mean coverage was estimated per window of 1000 bp from all individuals. The mean coverage per window (y axis) was spotted along the chromosomes (x axis). TB=Twist Bioscience, AG=Agilent

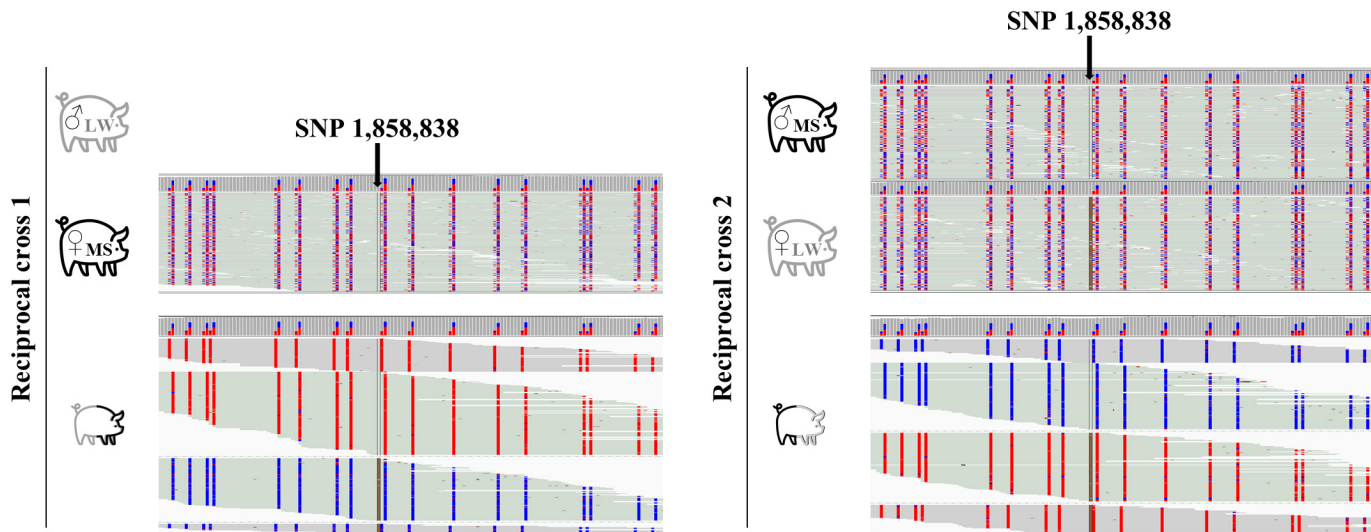
a

		SNP 1,384,751 - ICR1			ICR2 - SNP 1,858,838 - ICR2		
		genotype	M*	unM*	genotype	M*	unM*
Reciprocal cross 1	♂ LW						
	♀ MS	0/0			0/0		
	LWMS	1/0	1 pat	0 mat	1/0	0 mat	1 pat
	LWMS	1/0	1 pat	0 mat	1/0	0 mat	1 pat
Reciprocal cross 2	♂ MS	0/0			0/0		
	♀ LW	1/1			1/1		
	MSLW	0/1	0 pat	1 mat	0/1	1 mat	0 pat
	MSLW	0/1	0 pat	1 mat	0/1	1 mat	0 pat

b



c



Extended Data Fig.2: Detection of PofO methylation. **a**, Examples of informative variants from reciprocal crosses for which the parental origin is unambiguous. LW - Large White breed, MS - Meishan breed, LWMS - F1 offspring with half of the genome coming from a LW boar (paternal) and the second half coming from a MS sow (maternal), MSLW - F1 offspring with half of the genome coming from a MS boar (paternal) and the second half coming from a LW sow (maternal), ICR1 and ICR2 - Imprinting Control Regions 1 and 2, SNP - Single Nucleotide Polymorphism. **b**, **c**, Screenshots of the IGV browser (<https://software.broadinstitute.org/software/igv/>) focus on ICR1 (**b**) and ICR2 (**c**). Informative variants are shown with the arrow. Reads are grouped by allele at the SNP position and in the DNA methylation mode, converted CpGs (methylated) are represented in red and non-converted CpGs (unmethylated) are represented in blue.